Kütahya Dumlupınar University
Institute of Graduate Studies

Journal of Scientific
Reports-A
E-ISSN: 2687-6167
Number 53, June 2023

RESEARCH ARTICLE

THE ROLE OF MHD WAVES IN HEATING OF THE SOLAR CORONA

Ebru BAŞ[1], Dicle ZENGİN ÇAMURDAN[2,*]

[1] Department of Astronomy and Space Sciences, Faculty of Science, Ege University, 35100 İzmir, Turkey, ebru.1093.ebru@gmail.com, ORCID: 0000-0002-2055-0259
[2] Department of Astronomy and Space Sciences, Faculty of Science, Ege University, 35100 İzmir, Turkey, dicle.zengincamurdan@ege.edu.tr, ORCID: 0000-0003-2596-1775

Receive Date:02.11.2022 *Accepted Date: 14.05.2023*

ABSTRACT

The million-degree-temperature corona, which exists above the cooler photosphere layer, is an unsolved astrophysical phenomenon. Magnetohydrodynamic (MHD) waves have recently been the favored subject of heating of corona and driving the solar wind research. In order to acquire a better knowledge of wave heating,, we must consider how various dissipation parameters, such as viscosity, temperature anisotropy, and heat conduction can influence the evolution of these phenomena in the coronal plasma. It was recently discovered that plume and inter-plume lanes (PIPL) structure North Polar Coronal Hole (NPCH) in the radial direction, however this has not been taken into consideration in many studies. SOHO/UVCS satellite data show that some parameters (i.e., temperature, particle number density) are different in these regions. We aim to find that whether these regions affect the dispersion properties of the incompressible MHD waves. We assumed a model based on a process of Alfvén/ion cyclotron resonance with O VI ions by using quasi-linear approximation taking into account PL and IPL structre in NPCH, for the first time. Our results show that the damping length scales ($0.2 - 1.8\,R$) and energy flux densities ($\sim 10^6$ erg cm^{-2} s^{-1}) of Alfvén waves are identical for both plumes and interplumes in NPCH. This amount of energy is sufficient to heat the coronal hole and accelerate the solar wind above $2 - 6\,R$.

Keywords: *Solar corona, Magnetohydrodynamic, Alfvén waves, Solar wind.*

1. INTRODUCTION

The solar corona exhibits different characteristics at the different phase of solar cycle (i.e., a quiescent active region, a flaring active region, an equatorial and a polar coronal hole, etc.). As a result, magnetic field strength, temperature, particle number density, and other physical properties vary from one region to another. The temperature of the photosphere which is the inner solar atmosphere is 5780 K. However, the corona which is the outer atmosphere of the Sun is not an isolated layer, and there is mass and energy transfer in both directions between the inner and outer layers via a region known as the transition region, where a sharp shift in temperature is seen (from 20000 K in the upper

JSR A
Journal of Scientific Reports

chromosphere to over 2 MK in the corona) [1]. The main questions are that what process (or mechanisms) is (are) responsible for the coronal heating, and how can this solar atmosphere recover enough energy to maintain a temperature of more than one million K? This is a long-standing problem of solar physics for over sixty years.

Several heating mechanisms have been proposed since the observations revealed the coronal heating problem. These mechanisms are typically divided into models that use alternating current (AC) and direct current (DC). AC models contain mechanisms with the photospheric driving timescale (τ_{ph}) that are smaller than the Alfvén travel-time (τ_A) through a coronal loop and primarily comprise of wave dissipation models ([2], [3], [4]) and MHD Alfvén wave. In the DC models, the photospheric driving timescale that are longer than the Alfvén travel-time ($\tau_{ph} \gg \tau_A$) and the coronal magnetic field becomes tangled and braided by slow footpoint motions. According to these models, the magnetic energy is dissipated via nanoflares and small-scale reconnection events ([5], [6], [7]). A full review of the analytical and numerical studies performed is far beyond the scope of this paper, so we suggest readers interested in the specifics of the heating process to two recent review papers by Cranmer & Winebarger [8] and Viall et al. [9]. Instead, we focus on one of the AC mechanism known as MHD wave heating that is currently the most favoured.

The solar plasma at such temperature has a tendency to lose energy via optically thin radiation and thermal conduction and mass loss with the solar wind and solar activities (flares, mass ejections from corona), which are referred to as macroscopic processes. In addition, small-scale processes like viscosity, electrical resistance, heat conductivity, and forced vibration transmit energy from one area to another. Small-scale processes, referred to as dissipative in terms of energy and heat equations, result in the conversion of mechanical energy into heat and raise the entropy of the plasma. These processes, according to the MHD wave theory, transform mechanical energy stored in the wave's ordered motion into disordered thermal energy of the particles and can serve as a constant supply of energy for the corona. This study uses the propagation properties of these waves, which resonate with O VI ions, to investigate the coronal heating problem in NPCH by wave-particle interactions in the context of the MHD approximation.

Magnetic waves can dissipate their energy in the atmosphere, heating the corona and can be seen all over the corona. To explain the observations, several models have been developed. Extreme Ultraviolet (EUV) observations, performed by Transition Region and Coronal Explorer (TRACE) and the Solar and Heliospheric Observatory (SOHO) satellites, confirm the existence of MHD waves in NPCH ([10], [11], [12], [13], [14]). The line measurements observations of O VI and Mg X ions showed that beyond 1.75 - 2.1 R distance range, the solar plasma was collisionless in NPCH ([15]). These observations revealed the collisionless structure of the NPCH. This indicates that in the relevant distance extend, plasma transport processes should not be studied in the classical Coulomb collission. The ion-cyclotron resonance mechanism could be responsible for the extraordinarily large line widths. Therefore, the widths of the emission lines taken from this region can be used to understand how MHD waves contribute to heating the corona and increasing the speed of the solar wind. Observations of coronal lines formed at high temperatures ($T \geq 10^6$ K) from the solar edge along the radius direction to the solar corona ($R \geq 1.1\ R_\odot$). They provide confirmation for MHD-induced line

broadening. Hassler et al. [16] made the first observations in this field. They calculated the effects of opacity, systematic fluid effects, thermal Doppler expansion, and the effects of MHD waves on the line broadening using six EUV emission lines. They came to the conclusion that MHD waves may be reponsible for the non-thermal extraordinarily large line widths of the solar emission lines. In light of data from the Solar Maximum Mission (SMM) satellite's Flat Crystal Spectrometer (FCS), Saba and Strong [17] obtained a similar result. The SOHO satellite provided later work on measurements of the solar coronal emission lines. Doyle et al. [15] found Si VIII λλ 1440.49 and 1445.75 line widths as a measurement of location relative to the solar surface using SOHO/SUMER data. The non-thermal widths of the lines increased from ~ 24 km s^{-1} at the solar edge to ~ 28 km s^{-1} at a distance of 35 arcsec from the edge along the radius direction to the solar corona. Patsourakos and Klimchuk [18] demonstrated that non-thermal line broadening may be measured by examining the profiles of highly ionised lines such as Fe XVII. These observations have led them to the conclusion that MHD waves might be responsible for heating the quiescent solar corona. van Ballegooijen et al. [19]] investigated whether or not Alfvén wave turbulence can heat the corona and discovered that the photospheric waves can sustain a temperature of 2.5 MK. On the other hand, the nonthermal line broadening using Hinode/EIS observations was investigated by Brooks and Warren [20] and their findings contradict proposed models of coronal heating: nanoflares, Alfvén wave turbulence, reconnection.

The length and frequency of the damped waves provide guidelines for theoretical computations. Using Extreme Ultraviolet Imaging Telescope (EIT) and Ultraviolet Coronograph Spectrometer white-light channel (UVCS/WLC) measurements, Ofman et al. [21] examined the wave dampening in a gravitationally layered medium carried by a radially changing magnetic field. The damping of slow magnetosonic waves was calculated in this work to be 0.08 R under the compressive viscosity; however, for waves with a 300 s period, this value increases to 0.14 R ($R = r/R_{\odot}$, where $R_{\odot} = 7 \times 10^{10}$cm). They came to the conclusion that the dissipated waves might have an effect on the solar wind's acceleration and so transfer momentum to the collisionless region of the hole, which is located farther from the sun. The impact of nonlinear dissipation of Alfvén waves in coronal holes has been researched by Nakariakov et al. [22] and their results showed that short-period Alfvén waves (< 10 s) and the periods ~ 300 s become diminished within radial distances of $10\,R$ and $1\,R$, respectively. These waves may be responsible for the solar wind's acceleration as well as the heating of the coronal hole plasma. The periodicities and propagation speeds of MHD waves discovered in coronal hole structures were summarized in Table 1 by Banerjee et al. [23]. However, it seems that the related energy flow that the Alfvénic waves are thought to be carrying at the corona is enough to satisfy the requirements for acceleration of the solar wind and/or coronal plasma heating (also see Discussion section).

Furthermore, As can be seen in Fig. 1, the observations of Wilhelm et al. [24] show that NPCH is structured radially by plume lanes (PL) and interplume lanes (PIPL). These structures are considered by many studies ([21], [25], [26], [27]). Thermal conductivity, viscosity and anisotropic resistivity are found in the higher level of chromosphere and corona (see details in Sec. 2). The observed periods for the plume and inter-plume regions in this study are between $600 - 1800$ s. Using Doppler velocity time records of the corona, Morton et al. [27] studied Alfvén wave propagation through the solar atmosphere. Their research revealed the presence of forward- and backward-propagating Alfvén

JSR A
Journal of Scientific Reports

waves in plume (PL) and interplume (IPL) lanes, which are open magnetic field line regions. They noted the presence of turbulence in Alfvén wave, that heats the plasma and speeds up the solar wind. They were able to identify counter-propagating waves from the power spectra they obtained. In addition to this, Banerjee et al. [26] discovered that non-thermal velocities differ between plume and inter-plume plasma, with increased velocities measured in the inter-plume regions.

The goal of this study is to test the hypothesis that waves are indeed what heats the corona and propels the solar wind so both the damping lenght scale of the waves and the energy dissipated by the waves must be quantified. In the present work, we investigate the damping and propagation of Alfvén waves in NPCH in the context of incompressible MHD, and the basis for the current investigation is mainly given by Pekünlü et al. [28]. We investigate the dissipation of MHD waves taking into account the data from SOHO satellite on temperature, variations in non-thermal line widths and electron distribution in the PL/IPL structure of NPCH. The effects of the isotropic viscosity on the propagation characteristics of these waves are taken into account in the constructed model. In order to compute the damping length scales and wave energy flows, we rederive the dispersion relation. In this context, we will discuss the findings on how MHD waves accelerating solar wind and heating the corona. The novelty of our approach is that we focus on how the PL/IPL structure of NPCH affects wave propagation characteristics which has not been studied previously, using incompressible MHD waves.

The novelty of our approach is that we investigate the effect of the PL/IPL structure of NPCH on wave propagation characteristics, which has not been studied previously, using incompressible MHD waves. The propagation characteristics of incompressible MHD waves with periods of 0.0001 - 0.01 s within the range of 1.05 - 1.35 R were examined in the study by Pekünlü et al. [28], R is the radial distance that has no dimensions ($R = r/R_{\odot}$). Furthermore, in contrast to Pekünlü et al. [28], considering the recent literature studies, we chose waves having angular frequency $\omega = 0.01 - 1$ rad/s, that represents a period range of $628 \text{ sec} > P > 6.28$ sec in 1.65 - 3.50 R region.

2. PROPERTIES OF PLASMA and BASIC MODEL for NPCH

2.1. Number Densities in NPCH

Many studies have attempted to estimate the electron number density distribution in the coronal hole ([29], [30], [15], [31]). The measurements of Si VIII line ratio found that the densities of electron in the NPCH were approximately two times less than in low solar activity [32].

The electron number density is calculated for the range 1.65 - 3.50 R. Wilhelm et al. [33] reported that the coronal hole is typically constant, based on observations from many plume and interplume locations over the two Solar minimums. Since the mathematical relationship established by Doyle et al. [15] is compatible with the data of the electron number density change in the plume and interplume region, we used it in our investigation of electron number density variation,

$$N_e = \frac{1 \times 10^8}{r^8} + \frac{2.5 \times 10^3}{r^4} + \frac{2.9 \times 10^5}{r^2} \text{ cm}^{-3} \quad (1)$$

JSR A
Journal of Scientific Reports

relation is used. $R = r/R_{\odot}$ denotes the radial distance that is normalized. In NPCH, mass density is defined as $\rho_0(r) = \tilde{\mu}\, m_p N_e$, where m_p is the mass of proton mass and $\tilde{\mu}$~0.6 is the average atomic weight. According to Priest [34], the pressure scale height Λ_p is as follows:

$$\Lambda_p = 5.0 \times 10^6\, T(r)\, (r/R_{\odot})^2 \text{ cm} \tag{2}$$

NPCH is electrically quasineutral, which indicates that the amount of electrons is equal to the number of protons [35], [36], [37]. The number of electrons in PL is approximately 10 % greater than that in IPL [38].

In our work, we used Devlen and Pekünlü's [39] equation for the distribution of the numerical density of protons in the space of plume conditions, with $N_e = N_p$:

$$N_p^P(R,x) = N_p^{IPL}(R)\left(1 + 0.1\, Sin^2(2\pi x/92.16\, R)\right) \tag{3}$$

The abundances of some elements (such as oxygen) were measured in coronal streamers by Raymond et al. [40]. They discovered that the number density of oxygen is $N_{O\,VI} = 6.8 \times 10^{-5} N_p$. Cranmer et al. [41] provide the highest and lowest values changing between $2.4 \times 10^{-6} N_p - 8 \times 10^{-7} N_p$ in polar coronal holes.

2.2. Temperatures in NPCH

SOHO/UVCS data suggested that the NPCH is configured by bright and dim lanes [42]. According to their findings, the form of the NPCH is consisted of bright, cold, and high-intensity plumes (PL) and dim, warm, and low-intensity interplume bands (IPL). An collisionless plasma is most likely to exhibit temperature anisotropy. Using ion line of sight velocities, SOHO/UVCS data demonstrated that the temperature of the O VI ion observed near the coronal hole is direction dependant [43], [41]. In this condition, the kinetic temperature of ion in the perpendicular direction to the magnetic field, $T_{\perp}$, is higher than its temperature in the parallel direction, $T_{\parallel}$. UVCS data revealed comparable temperature dependences for other rare ions in the coronal hole (He++, Si VIII, Mg X, and etc). The emission line lengths of O VI ions measured in IPL were found to be wider than those measured in PL. This suggests that heating interplume lanes perpendicular to magnetic field lines is more effective than heating plumes [44], [33]. These findings suggest that the ion-cyclotron induced vibration method can heat the coronal plasma.

Because there are no observational data on the temperature distribution of the plasma in NPCH, the temperature is assumed to be isothermal along the line of sight. the temperature along los is considered to be isothermal. On the other hand,, Kohl et al. [43] discovered that O VI line intensity changed in both the radial and x directions.

JSR A
Journal of Scientific Reports

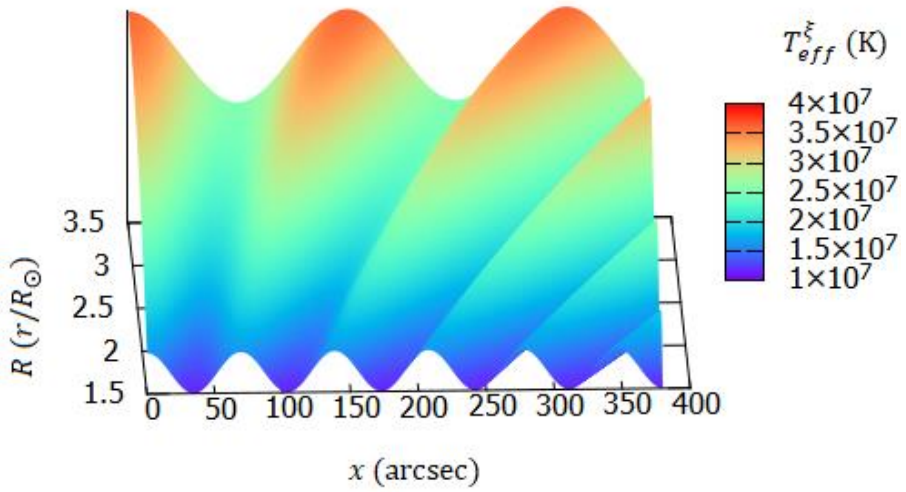

Figure 1. T_{eff}^{ξ} values of the O VI ions depending on the parameters R and x. Wave crests correspond to warmer IPL, and troughs between two ridges correspond to cooler PL in the NPCH. The width of the PIPL change with R. The axis x is measured in arcseconds, as it is in [22]. This figure is reproduced with permission of Devlen et al. [46].

The relationship between ion temperature and effective temperature is identified by Wilhelm et al. [42]

$$T_{eff} = \frac{m_i}{2k_B} v_{1/e}^2 = T_i + \frac{m_i}{2k_B} \xi^2 \tag{4}$$

where the Boltzmann constant, the mass and temperature of ion are denoted by k_B, m_i , T_i , respectively. The most likely velocity of an ion through the los is showed $v_{1/e}$. In an isotropic turbulent velocity field with Gaussian distributions, ξ represents the speed that has the highest likelihood of occurrence based on the probability density function. Esser et al. [45] defined the relation between wave amplitude and ξ, $\langle \delta v^2 \rangle = 2\xi^2$.

According to Wilhelm et al. [42], T_{eff} (O VI) in IPL is approximately 30% greater than that of PL. The two-dimensional effective temperature calculated by Devlen et al. [26] was used in our study based on this observation. Figure 1 illustrates the observed variation as well.

According to Devlen and Pekünlü [39],

$$T_{eff}(R) = -7.941 \times 10^7 R^2 + 4.9487 \times 10^8 R - 5.7625 \times 10^8 \tag{5}$$

JSR A
Journal of Scientific Reports

Table 1. The effective temperature (T_{eff}), the ion temperature (T_i), and the component of the effective temperature that is not related to thermal processes (T_{eff}^{ξ}) in the interplume and plume region for O VI ion, are presented as an expression of distance along the radial axis (R). Temperature units are 10^7 K.

	Interplume			***Plume***		
$\boldsymbol{R}$	$\boldsymbol{T_{eff}}$	$\boldsymbol{T_i}$	$\boldsymbol{T_{eff}^{\xi}}$	$\boldsymbol{T_{eff}}$	$\boldsymbol{T_i}$	$\boldsymbol{T_{eff}^{\xi}}$
1.7	3.55	1.61	1.94	2.49	1.13	1.36
1.8	5.72	3.62	2.10	4.01	2.54	1.47
1.9	7.73	5.48	2.26	5.46	3.86	1.59
2.0	9.58	7.18	2.40	6.83	5.12	1.71
2.1	11.28	8.74	2.54	8.14	6.31	1.83
2.2	12.81	10.15	2.66	9.37	7.43	1.95
2.3	14.19	11.40	2.78	10.53	8.47	2.07
2.4	15.40	12.51	2.90	11.60	9.42	2.18
2.5	16.46	13.46	3.00	12.58	10.28	2.29
2.6	17.36	14.26	3.10	13.45	11.05	2.40
2.7	18.10	14.92	3.18	14.21	11.71	2.50
2.8	18.68	15.42	3.26	14.85	12.25	2.59
2.9	19.10	15.77	3.34	15.36	12.68	2.68
3.0	19.37	15.97	3.40	15.75	12.99	2.77
3.1	19.47	16.02	3.46	16.00	13.16	2.84
3.2	19.42	15.91	3.50	16.12	13.21	2.91
3.3	19.20	15.66	3.54	16.09	13.12	2.97
3.4	18.83	15.26	3.58	15.91	12.89	3.02
3.5	19.30	14.70	3.60	15.59	12.52	3.07

The value ranges of ξ for Mg X and O VI ions are precisely comparable to one another and change in the identical direction as R, as revealed by Esser et al. [45]. Taking all of this into consideration, Devlen and Pekünlü [39] calculated a polynomial expression for the component of the effective temperature that is not related to thermal processes of O VI ions using Mg X data for ξ, which we use in our study, as shown below.

$$T_{eff}^{\xi} = -4 \times 10^6 R^2 + 3 \times 10^7 R - 2 \times 10^7 \tag{6}$$

$$T_{eff}^{P}(R, x) = T_{eff}^{IPL}(R)\left(1 + 0.3\, Sin^2(2\pi x / 92.16\, R)\right) \tag{7}$$

In this study, we calculated the variations of T_{eff}, T_i, T_{eff}^{ξ} with radial distance using Equations (5)-(7) for both plume and interplume lanes, which are listed in Table 1.

JSR A
Journal of Scientific Reports

2.3. The Solar Magnetic Field Intensity in NPCH

The magnetic field (B) variation with R in NPCH as determined by Hollweg [47] is given in Equ. 8. Because there is no data in the literature on how B varies in the PL and IPL, in particular with respect to the x direction, we will suppose that the following formula employs to both PL and IPL.

$$B = 1.5(f_{max} - 1)R^{-3.5} + 1.5R^{-2} \text{ G} \tag{8}$$

with $f_{max} = 9$.

3. MHD EQUATIONS

The equations of motion, magnetic flux conservation, and magnetic induction are the fundamental equations for the propagation of waves and dissipation within an incompressible fluid. [48]:

$$\rho \frac{D\mathbf{v}}{Dt} = (\nabla \times \mathbf{B}) \times \frac{\mathbf{B}}{\mu} + \rho v \left[\frac{4}{3}\nabla(\nabla \cdot \mathbf{v}) - \nabla \times \nabla \times \mathbf{v}\right] \tag{9}$$

$$\frac{\partial \mathbf{B}}{\partial t} = \nabla \times (\nabla \times \mathbf{B}) + \eta \nabla^2 \mathrm{B} \tag{10}$$

$$\nabla \cdot \mathbf{B} = 0 \tag{11}$$

In these equations, B , v , ρ represent the magnetic field vector, the fluid velocity, the mass density of gas and v , μ represent kinematic viscosity and magnetic permeability. $\eta = 5.2 \times 10^{11} T^{-3/2} \ln \Lambda$ $\mathrm{cm^2\ s^{-1}}$ refers magnetic diffusivity.

The viscosity coefficient is given by Spitzer [49],

$$\rho v = 2.21 \times 10^{-15} \frac{T^{5/2}}{ln\Lambda} \text{ g cm}^{-1}\text{s}^{-1} \tag{12}$$

here $ln\Lambda\ (= 22)$ represents the Coulomb logarithm.

$$D/Dt = \partial/\partial t + \mathrm{v} \cdot \nabla \tag{13}$$

represent the Lagrangian derivative.

We applied a conventional WKB (Wentzel-Kramers-Brillouin) perturbation analysis to examine the equilibrium state. All variables are represented in this examination by adds of equilibrium and a minor perturbed quantity where "0" and "1" subscript indicates these parameters, respectively, i.e. $\rho = \rho_0 + \rho_1$, $\mathrm{B=B_0 + B_1}$ etc.

The linearized equations derived from Eq. 8 - Eq.10 are as follows:

JSR A
Journal of Scientific Reports

$$\rho_0 \frac{D\mathrm{v_1}}{Dt} = \frac{1}{\mu}(\mathrm{B_0}\cdot\nabla)\mathrm{B_1} + \rho_0 v\nabla^2\mathrm{v_1} \tag{14}$$

$$\frac{\partial \mathrm{B_1}}{\partial t} = (\mathrm{B_0}\cdot\nabla)\mathrm{v_1} + \eta\nabla^2\mathrm{B_1} \tag{15}$$

$$\nabla\cdot\mathrm{B_1} = 0 \tag{16}$$

Perturbed values are generally thought to be small in compared to equilibrium values in the linear approximation., i.e. $\rho_1\cdot\rho_1 = 0$ and $\mathrm{B_1}\cdot\mathrm{B_1} = 0$ etc.

We assume that the perturbation quantities vary as $\exp[i(\mathbf{k}.\mathrm{r} - \omega t)]$. For Eq. 14 - Eq.16, we use the following replacements: $\partial/\partial t \rightarrow -i\omega$ and $\nabla \rightarrow ik$. We applied scalar product Eq. 14 - Eq.16 with $\widehat{\mathrm{B_0}}$ unit vector;

$$\rho_0(i\omega)\left(\mathrm{v_1}\cdot\widehat{\mathrm{B_0}}\right) + \frac{1}{\mu}i(\mathrm{B_0}\cdot\mathbf{k})\left(\mathrm{B_1}\cdot\widehat{\mathrm{B_0}}\right) - v\rho_0 k^2\left(\mathrm{v_1}\cdot\widehat{\mathrm{B_0}}\right) = 0 \tag{17}$$

$$(i\omega)\left(\mathrm{B_1}\cdot\widehat{\mathrm{B_0}}\right) + i(\mathrm{B_0}\cdot\mathbf{k})\left(\mathrm{v_1}\cdot\widehat{\mathrm{B_0}}\right) - \eta k^2\left(\mathrm{B_1}\cdot\widehat{\mathrm{B_0}}\right) = 0 \tag{18}$$

We can derive the dispersion relation from equations (17) and (18) as follows:

$$\eta v k^4 + \left({v_A}^2 - i\omega(v+\eta)\right)k^2 - \omega^2 = 0 \tag{19}$$

where $v_A = B_0/\sqrt{\mu\rho_0}$ is Alfvén velocity.

We solved the equation (19) numerically using Matlab code, and we get two different complex values of k (wave number), negative and positive of the same value. A negative value for k indicates that the wave is damped as it propagates outward from the sun. Reversing the imaginary part of the smaller k value yielded the wave's damping length scale.

For the range of 1.65-3.50 R, the wave energy flux density is calculated using Priest's [48] formula.

$$F = \rho\langle\delta v^2\rangle\frac{\partial\omega}{\partial k} \tag{21}$$

where $\partial\omega/\partial k$ is the wave's group velocity, and $\langle\delta v^2\rangle = 2\xi^2$ corresponds to the non-thermal part of the velocity which is related to fine-scale turbulent structures that remain unresolved [39].

The polynomial function provided by Esser et al. [45] was used by Devlen and Pekünlü [39] to express the non-thermal velocities of OVI ions as follows:

$$\xi = 0.2\times10^7 R^3 - 10^7 R^2 + 4\times10^7 R - 3\times10^7 \tag{22}$$

JSR A
Journal of Scientific Reports

Table 2. The energy flux density and length scale for damping of Alfvén waves of different periods propagating along a plume in the radial direction of R. x is chosen 40″ for plotting purpose. The viscosity value was assumed as 10^{20} cm^2 s^{-1} in the calculations.

P (s)	R	$1/k_i$ ($R_\odot$)	F(erg cm^{-2} s^{-1})
6	1.6	0.1983	1.01×10^7
	1.8	0.1983	6.79×10^6
	2.0	0.1983	4.70×10^6
	2.2	0.1982	3.45×10^6
	2.4	0.1982	2.72×10^6
	2.6	0.1982	2.31×10^6
	2.8	0.1983	2.10×10^6
	3.0	0.1983	2.01×10^6
60	1.6	0.6207	3.20×10^6
	1.8	0.6196	2.15×10^6
	2.0	0.6186	1.49×10^6
	2.2	0.6180	1.09×10^6
	2.4	0.6179	8.61×10^5
	2.6	0.6182	7.31×10^5
	2.8	0.6188	6.63×10^5
	3.0	0.6197	6.37×10^5
600	1.6	1.8142	1.04×10^6
	1.8	1.7977	7.05×10^5
	2.0	1.7855	4.93×10^5
	2.2	1.7785	3.64×10^5
	2.4	1.7768	2.87×10^5
	2.6	1.7802	2.43×10^5
	2.8	1.7883	2.19×10^5
	3.0	1.8003	2.09×10^5

The wavelength $\lambda(= 2\pi/k_r)$ is compared with the value of the local pressure scale height (Λ_p). The scientific reliability of the "slowly varying medium" approach is examined for preferred frequencies and radial distances. We obtained that the criterion of "slowly varying medium", namely $\lambda/\Lambda_p \ll 1$, is satisfied for the period less than 60 s in the considered radial range. One should, however, keep in mind that this condition is not satisfied for the periods, $P > 60$ s. Nonetheless, we consider them worthy of use because the observations have unambiguously shown that these waves are present in the NPCH [22],[23]. However, one should take caution when interpreting the results from this study for waves with longer periods.

Because viscosity coefficient is not well-constrained in the conditions of the solar corona, we need to specify that we adopted this coefficients as a free parameter.

JSR A
Journal of Scientific Reports

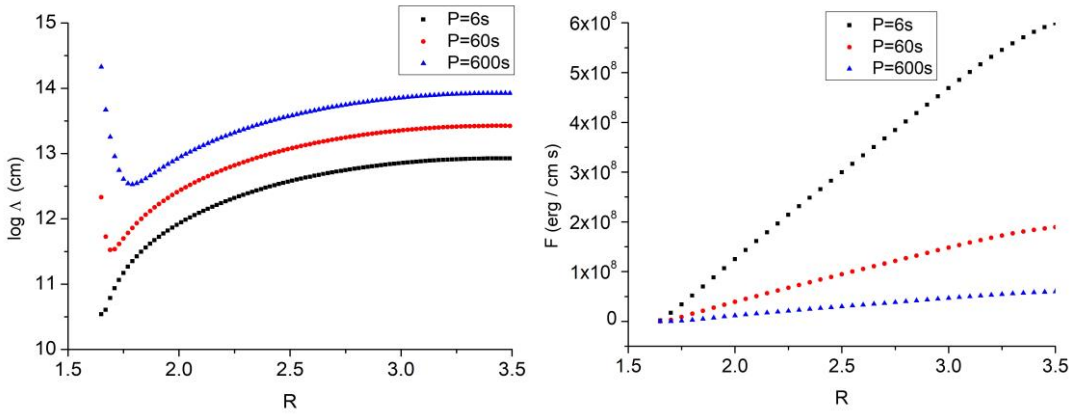

Figure 2. Comparison the damping length scale $(1/k_i)$ with R, where k_i is the imaginary part of the wave vector. The variation of the wave energy flux density with respect to R normalized radial distance is showed in bottom pannel.

4. DISCUSSION

In a collisionless plasma, like the NPCH region in sun, the effectiveness of Alfvén waves in heating and the propagation characteristics has not yet been studied in detail. We tried to comprehend to understand how ions such as O VI react to the propagation of these waves within NPCH as far as 1.5 – 3.5 R at frequencies that are close to their cyclotron frequency in this study. In addition to this, assuming that the solar plasma is an incompressible plasma, we examine the impact of the PL/IPL formation of coronal hole on the properties of wave propagation which has never been investigated before.

The first step in the study is to compute the length scales for damping and to determine whether the waves with the appropriate value have the required energy that will cause coronal heating and the solar wind's acceleration. In the context of incompressible MHD, for ω was given a value in the range $6 < P < 600$ covering the radial distance of 1.5– 3.5 R, we investigate how the ion-cyclotron waves propagate. The variation in length scale for damping $(1/k_i)$ of the wave obtained using Equ. (19) and Figure 2 presents the variation of this parameter in solar radius as a function of radial location relative to the sun (left). According to Fig. 2 (left), as the wave period increases, so does the damping length scale. The figure shows that that R also causes an increase in the wave's damping length scale. Figure 2 (right) demonstrates the change in energy flux density of the waves as a function of radial location relative to the sun. It is evident that the waves's energy flux density increases with increasing radial distance and decreases with increasing wave period. The length scale for damping of the high frequency waves has larger values ($> 5\ R$), as can be seen in Fig. 2 (left).

We made the first attempt to build a numerical solution of the dispersion relation for these waves to comprehend the properties of MHD wave propagation along the plume and interplume structure. For

JSR A
Journal of Scientific Reports

this purpose, we calculated the energy flux densities and damping length scales in the radially using $x = 40''$ as the plume's midpoint distance. Assuming viscosity has a value of 10^{20} cm^2 s^{-1}, at some radial distances, Table 2 shows the calculated parameters of waves for periods 6,60 and 600 s. As can be seen in the Table 2, as distance increases, the fluxes tend to decrease and this decrease in flux is more significant at shorter periods.

Figure 3 illustrates how frequency and viscosity effects variations in the energy flux density (bottom) and the length scale for damping (top) of a waves in a plume at $R = 1.7\ R$. We used false colors in this figure that display length-scales from 0.01 to 6.5 R (top figure) and the logaritmic energy flux density of the waves (Log *F)* between 5.5 and 8.5 (bottom figure). Viscosity is observed to rise linearly with frequency. For example, the damping length scale is $\sim 2.5 - 3\ R$ when the viscosity value is approximately 10^{21} cm^2 s^{-1} and the period of the wave is ~ 60 s, i.e., the logarithmic frequency is -1.0 s^{-1}. Since the viscosity coefficient in coronal conditions is uncertain, it appears that it is a crucial parameter in determining the distance at which the waves are damped, and for these waves that plays a role to the coronal's heating, its value should be greater than 10^{20} cm^2 s^{-1}.

Studies suggest that for appropriate values of damping scale length, an energy flux density of MHD waves roughly $10^6 - 10^7$ erg cm^{-2} s^{-1} is sufficient. The energy flux density of the wave is observed to increase with increasing viscosity when the frequency is fixed at a specific value. These waves have identical length scales for dissipation and energy flux densities for plumes and interplumes. On the other hand, as suggested by Cranmer et al. [44], the heating interplume lanes perpendicular to magnetic field lines is more effective than heating plumes. Similarly, Dogan and Pekunlu [50] obtained that the resonance mechanism in the IPL is far more effective than in the PL using a model based on the kinetic theory. However, we could not find any evidence that the resonance mechanism works more efficiently in any of these regions. We consider that the incompressible plasma assumption for NPCH in our model may not be valid for this region, or the variations between the PL and IPL regions can be revealed by taking into account different ion contributions in the modelling as opposed to heating with the only O VI ion.

In Figure 4, when waves with a wider period range ($P = 0.0001 - 600$ sec) are examined at $R = 1.7\ R$, it is noticed that L values of these waves is in the range of 1-1.5 R for all frequencies when the viscosity is $< 10^{20}$ cm^2 s^{-1}. The L is greater than $2\ R$ for the frequency range of $0.001 - 100$ s^{-1} when the viscosity value is greater than 10^{20} cm^2 s^{-1}. At higher frequencies, the L value is less than $1.5\ R$.

JSR A
Journal of Scientific Reports

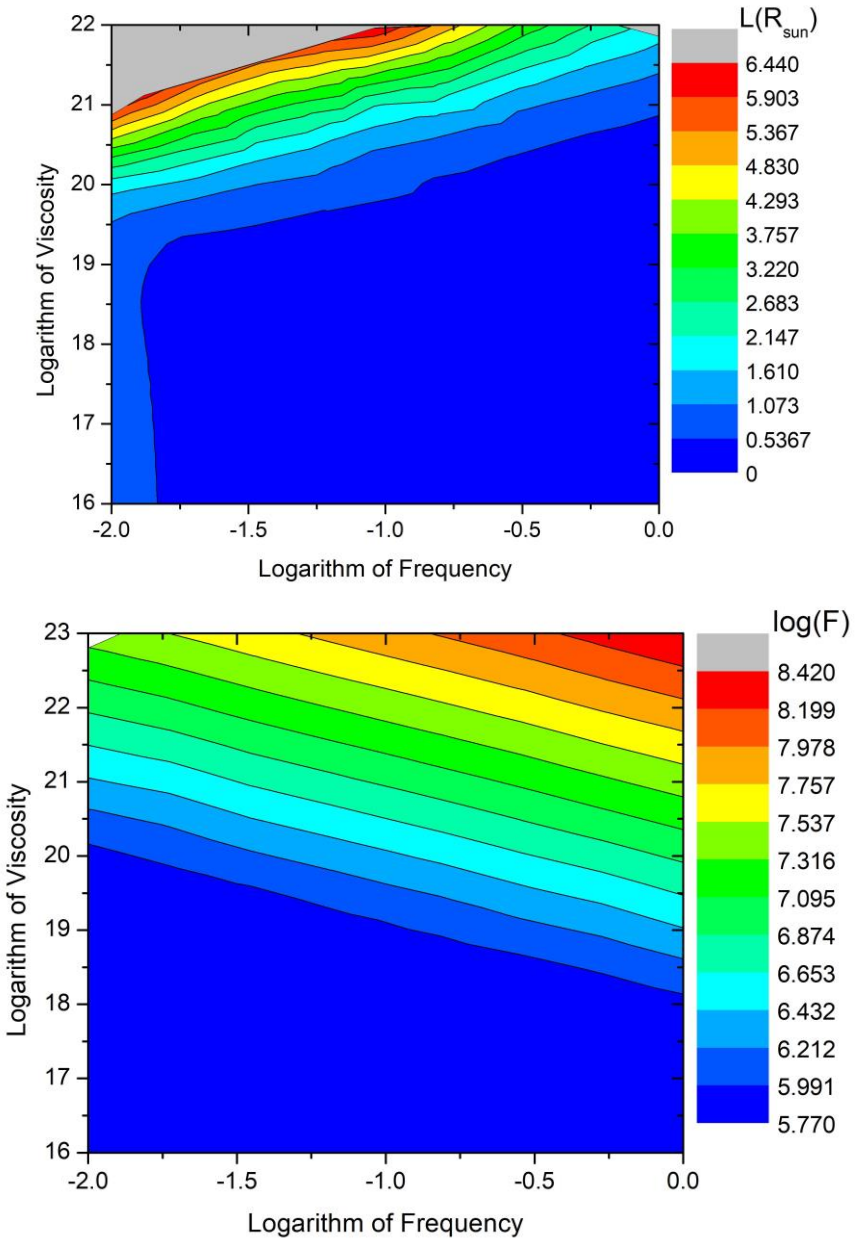

Figure 3. The length-scale for damping contours in R_{sun} unit (top) and flux densities (bottom) shown versus viscosity and frequency in logaritmic scales in the case of waves transmitting in a plume.

JSR A
Journal of Scientific Reports

Table 2 shows that the waves's flux densities continuously reduce as the radial direction increases. This energy decay suggests that waves and ions in plume structure in coronal hole are exchanging energy through ion cyclotron resonance process. The literature provides some information concerning energy fluxes and the wave's length scales for damping and is used to compare the results obtained in our study (see Table 3). According to Hollweg [51] and Hollweg and Johson [52], the essential energy density flux for heating the corona is 5×10^5 erg cm^{-2} s^{-1}. According to [53], 8×10^5 erg cm^{-2} s^{-1} is the MHD wave energy flux needed for heating this region. McIntosh et al. [54] examined spectral observations from the Solar Dynamics Observatory's (SDO) Atmospheric Imaging Assembly (AIA). They discovered that small amplitude waves in a NPCH region contain enough energy to account for the heating needs of coronal holes ($1 - 2 \times 10^5$ erg cm^{-2} s^{-1}). Magnetic wave energy dissipation is important not just for coronal heating in coronal holes, but also for the acceleration of the fast solar wind (for details see [55], [23]). According to Hahn et al. [56], the observed fast decline in line widths is needed to heat the NPCH and promote the solar wind acceleration. Hahn and Savin [57] calculated the energy flow density to be 6.7×10^5 erg cm^{-2} s^{-1}. In addition to this, anisotropic heat conduction and isotropic viscosity effects on MHD wave propagation in the NPCH were examined by Devlen et al. [46] for compressible MHD waves. Their findings demonstrate that the wave propagation characteristics are novelly introduced by the perpendicular heat conduction. Alfvén waves have energy flux densities that range from $10^6 - 10^{8.6}$ erg cm^{-2} s^{-1}. Their findings imply that transformed magnetoacoustic waves might be the primary driver of the O VI ion heating and preferential acceleration that has been observed, as well as an additional accelarator concerning the fast solar wind in this region.

The these waves's flux densities in our investigation were calculated to be an interval of $10^5 - 10^7$ erg cm^{-2} s^{-1}, as indicated in Table 2. For example, L and F are $2\,R$ and 1.5×10^6 erg cm^{-2} s^{-1} respectively, for $P = 60$ s and viscosity coefficient around Spitzer value (10^{20} cm^2 s^{-1}). Our findings imply that Alfvén waves deposit energy in the NPCH, supplying as a critical resource of heating this layer and primarily favored heating of oxygen ions. This quantity is expected to replace the energy lost in NPCH due to heat conduction to lower regions and optically thin emission.

Table 3. An overview of some of the research on the waves's energy flux density in various areas of solar corona.

Region	$\boldsymbol{F}$(erg cm^{-2} s^{-1})	**References**
Coronal Hole	8×10^5	Withbroe & Noyes [53]
Corona	4-5 $\times 10^5$	Hollweg [51] Hollweg &Johson [52]
NPCH	5×10^5	Banerjee et al. [31]
Coronal Hole	1-2 10^5	McIntosh et al. [54]
Polar Coronal Hole	6.7×10^5	Hahn & Savin [57]
NPCH	$10^6 - 10^{8.6}$	Devlen et al. [46]
NPCH	$10^5 - 10^7$	This study

JSR A
Journal of Scientific Reports

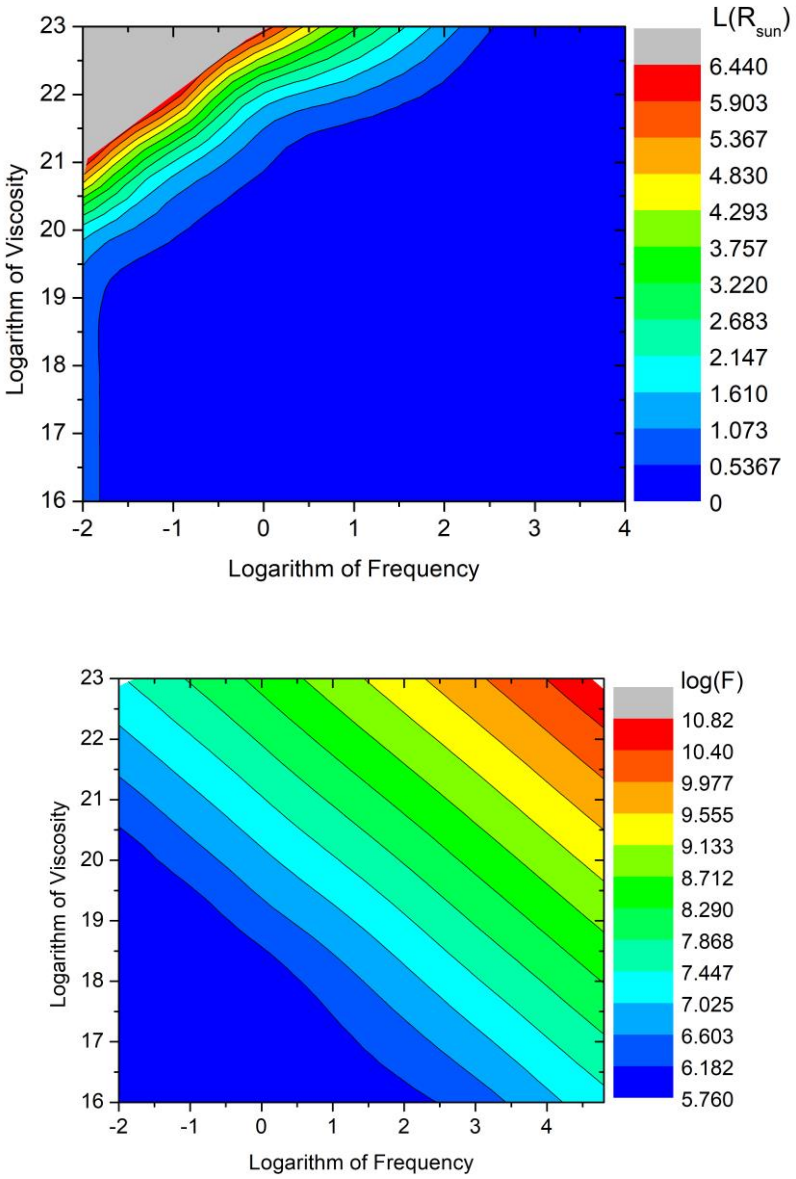

Figure 4. The length-scale for damping contours in R_{sun} unit (top) and flux densities (bottom) shown versus viscosity and frequency in logaritmic scales in the case of waves transmitting in a plume. The frequency range is between 0.0001 sec < *P* < 600 sec.

As shown by Antonucci et al. [58], coronal UVCS data can be utilized to detect an acceleration of the solar wind beyond $1.5 - 2\ R$. The data collected indicates the presence of compelling evidence of the fast solar wind within the central region of polar coronal holes, following the path of exposed magnetic fields. According to Telloni et al. [59], it is stated that Alfvén waves that are in resonance with ions cause energy dissipation in the outer corona across the magnetic field at a maximum rate around $1.9\ R$ which means the energy release can contribute to increase the wind speed. As a results, according to our findings, Alfvén waves have a greater damping length-scale ($2 - 6\ R$), Alfvén waves both in PL and IPL may be responsible for the extra the enhanced velocity of the fast solar wind that has been observed.

5. CONCLUSION

Our model, for the first time, takes into account the MHD wave propagation characteristics assuming an incompressible coronal plasma taking into account PL/IPL region in NPCH. Our investigation of the effect of the PL/IPL structure on Alfvén wave propagation characteristics yielded such results that the transmitting Alfvén waves's lenght scales for damping and energy flux densities along the Pl and IPL regions are remarkably similar. Alfvén waves with periods less than 60 seconds can contribute to and accelerate the solar wind beyond a heliocentric range of $2\ R$ and transport sufficient energy flux to heat this region. The Alfvén waves's propagation properties in NPCH show results that these waves possess sufficient energy flux to heat the corona. The wave mechanical flux density is in the order of 10^6 erg cm^{-2} s^{-1}. It is possible that the longer dissipation length-scale of these waves, which exist in both in both PL and IPL, is contributing to the measured increase in speed of the fast solar wind.
Various studies on the solar corona clearly show that this region's heating is not solely caused by the MHD wave dissipation. There are definitely various proposed mechanism at work, each with a different efficiency, in various areas of the solar corona. These include small-scale reconnection, the drifting of heating layers in phase mixing/resonant absorption known as nanoflare heating event, and others.

In order to solve the heating problem, we need improved observations. In the near future, new telescope and instrument data will soon provide high quality observations of the solar atmosphere. Recognizing the properties of coronal hole plasma will advantage from upcoming measurements of electron temperatures in the corona using the Solar Orbiter's SPICE spectrometer or polarimetric studies of the magnetic field in the corona utilizing the Daniel K. Inoue Solar Telescope. With the availability of additional data, we intend to improve our model for NPCH. The plasma fluid description in our model is a rough approximation to the coronal condition. The model we constructed in this study will be utilized to examine the wave dissipation characteristics in NPCH applying the solution of the collisionless Vlasov equation.

ACKNOWLEDGEMENT

This work is a part of the study of the MS thesis of E. Baş

REFERENCES

[1] Wedemeyer-Böhm, S., Lagg, A. , Nordlund, A., (2009), The Origin and Dynamics of Solar Magnetism, Space Sciences Series of ISSI, Volume 32. ISBN 978-1-4419-0238-2, Springer New York, p. 317.

[2] Ofman, L., Davila, J. M., Steinolfson, R. S.,(1994), Nonlinear studies of coronal heating by the resonant absorption of Alfvén waves, Geophysical Research Letters, Volume 21, Issue 20, p. 2259-2262.

[3] Pagano, P., De Moortel, I., (2017), Contribution of mode-coupling and phase-mixing of Alfvén waves to coronal heating, Astronomy & Astrophysics, Volume 601, id.A107, 13 pp.

[4] Pagano, P., Pascoe, D. J., De Moortel, I., (2018), Contribution of phase-mixing of Alfvén waves to coronal heating in multi-harmonic loop oscillations, Astronomy & Astrophysics, Volume 616, id.A125, 12 pp.

[5] Cargill, Peter J., Klimchuk, James A., (2004), Nanoflare Heating of the Corona Revisited, The Astrophysical Journal, Volume 605, Issue 2, pp. 911-920.

[6] Klimchuk, J. A., (2006), On Solving the Coronal Heating Problem, Solar Physics, Volume 234, Issue 1, pp.41-77.

[7] Chitta, L. P., Peter, H., Solanki, S. K., (2018), Nature of the energy source powering solar coronal loops driven by nanoflares, Astronomy & Astrophysics, Volume 615, id.L9, 6 pp.

[8] Cranmer, S. R., Winebarger, A. R., (2019), The Properties of the Solar Corona and Its Connection to the Solar Wind, Annual Review of Astronomy and Astrophysics, vol. 57, p.157-187.

[9] Viall, N. M., De Moortel, I.,Downs, C., Klimchuk, J. A., Parenti, S., Reale, F., (2021), The Heating of the Solar Corona, Space Physics and Aeronomy, Volume 1, Solar Physics and Solar Wind, Geophysical Monograph Series, Vol. 258. ISBN: 978-1-119-50753-6, 320 pp. American Geophysical Union, Wiley, 2021, p.35.

[10] Tomczyk, S., McIntosh, S. W., Keil, S. L., Judge, P. G., Schad, T., Seeley, D. H., Edmondson, J., (2007), Alfvén Waves in the Solar Corona, Science, Volume 317, Issue 5842, pp. 1192.

[11] Landi, E., Cranmer, S. R., (2009), Ion Temperatures in the Low Solar Corona: Polar Coronal Holes at Solar Minimum, The Astrophysical Journal, Volume 691, Issue 1, pp. 794-805.

[12] Gupta, G. R., Banerjee, D., Teriaca, L., Imada, S., Solanki, S, (2010), Accelerating Waves in Polar Coronal Holes as Seen by EIS and SUMER, The Astrophysical Journal, Volume 718, Issue 1, pp. 11-22.

[13] Bemporad, A., Abbo, L., (2012), Spectroscopic Signature of Alfvén Waves Damping in a Polar Coronal Hole up to 0.4 Solar Radii, The Astrophysical Journal, Volume 751, Issue 2, 110, 13 pp.

[14] Cranmer, S. R., Gibson, S. E., Riley, P., (2017), Origins of the Ambient Solar Wind: Implications for Space Weather, Space Science Reviews, Volume 212, Issue 3-4, pp. 1345-1384.

[15] Doyle J., Teriaca L., Banerjee D., (1999), Coronal hole diagnostics out to 8 R. Astronomy and Astrophysics, 349, 956.

[16] Hassler D. M., Rottman G. J., Shoub E. C., Holzer T. E., (1990), Line broadening of MG X 609 and 625 A coronal emission lines observed above the solar limb. The Astrophysical Journal, 348, L77-80.

[17] Saba J. L., Strong K. T., 1991. Coronal dynamics of a quiescent active region. The Astrophysical Journal, 375, 789-799.

[18] Patsourakos, S., Klimchuk, J. A., (2006), Nonthermal Spectral Line Broadening and the Nanoflare Model, The Astrophysical Journal, Volume 647, Issue 2, pp. 1452-1465.

[19] van Ballegooijen, A. A., Asgari-Targhi, M., Voss, A., (2017), The Heating of Solar Coronal Loops by Alfvén Wave Turbulence, The Astrophysical Journal, Volume 849, Issue 1, article id. 46, 23 pp.

[20] Brooks, David H., Warren, Harry P., (2016), Measurements of Non-thermal Line Widths in Solar Active Regions, The Astrophysical Journal, Volume 820, Issue 1, article id. 63, 14 pp.

[21] Ofman L., Nakariakov V., Sehgal N., (2000) Dissipation of slow magnetosonic waves in coronal plumes. The Astrophysical Journal, 533, 1071.

[22] Nakariakov V. M., Ofman L., Arber T. D., (2000), Nonlinear dissipative spherical Alfvén waves in solar coronal holes. The Astronomy and Astrophysics, 353, 741-748.

[23] Banerjee D., Gupta G. R., Teriaca L., (2011) Propagating MHD Waves in Coronal Holes. Space Science Reviews, 158, 267-288.

[24] Wilhelm K., Marsch E., Dwivedi B. N., Hassler D. M., Lemaire P., Gabriel A. H., Huber M. C., (1998), The solar corona above polar coronal holes as seen by SUMER on SOHO. The Astrophysical Journal, 500, 1023.

[25] Ruderman, M. S., Oliver, R., Erdélyi, R., Ballester, J. L., Goossens, M., (2000), Slow surface wave damping in plasmas with anisotropic viscosity and thermal conductivity, Astronomy and Astrophysics, v.354, p.261-276.

[26] Banerjee, D., Pérez-Suárez, D., Doyle, J. G., (2009), Signatures of Alfvén waves in the polar coronal holes as seen by EIS/Hinode, Astronomy and Astrophysics, Volume 501, Issue 3, 2009, pp.L15-L18.

[27] Morton R., Tomczyk S., Pinto R., 2015. Investigating Alfvénic wave propagation in coronal open-field regions. Nature Communications, 6, 1-12.

[28] Pekünlü E. R., Bozkurt Z., Afsar M., Soydugan E., Soydugan F., (2002), Alfvén waves in the inner polar coronal hole. Monthly Notices of the Royal Astronomical Society, 336, 1195-1200.

[29] Fisher R., Guhathakurta M., (1995), Physical properties of polar coronal rays and holes as observed with the Spartan 201-01 coronagraph. The Astrophysical Journal Letters, 447, L139.

[30] Guhathakurta M., Fisher R., (1998), Solar Wind Consequences of a Coronal Hole Density Profile: Spartan 201-03 Coronagraph and Ulysses Observations from 1.15 R to 4 AU. The Astrophysical Journal Letters, 499, L215.

[31] Banerjee D., Teriaca L., Doyle J., Wilhelm K., (1998), Broadening of SI VIII lines observed in the solar polar coronal holes. Astronomy and Astrophysics, 339, 208-214.

[32] Doschek G., Warren H., Laming J., Mariska J., Wilhelm K., Lemaire P., Schühle U., Moran T., (1997), Electron densities in the solar polar coronal holes from density-sensitive line ratios of Si VIII and Sx. The Astrophysical Journal Letters, 482, L109.

[33] Wilhelm K., Abbo, L., Aucre, F., and et al., (2011), Morphology, dynamics and plasma parameters of plumes and inter-plume regions in solar coronal holes. The Astronomy and Astrophysics Review, 19, 35.

[34] Priest E., Kirk J., Melrose D., (1994), Plasma astrophysics. Berlin: Springer-Verlag.

[35] Marsch E., (1999), Solar wind models from the Sun to 1 AU: Constraints by in situ and remote sensing measurements. Coronal holes and solar wind acceleration, 1–24.

[36] Endeve E., Leer E., (2001), Coronal heating and solar wind acceleration; gyrotropic electron-proton solar wind. Solar Physics, 200, 235-250.

[37] Voitenko Y., Goossens M., (2002), Excitation of high-frequency Alfvén waves by plasma outflows from coronal reconnection events. Solar Physics, 206, 285-313.

[38] Cranmer S. R., Kohl, J.L. and Noci, G. And et al., (1999), An empirical model of a polar coronal hole at solar minimum. The Astrophysical Journal, 511, 481.

[39] Devlen E., Pekünlü E. R., (2010), MHD waves in the solar north polar coronal hole. Astronomische Nachrichten, 331, 716-724.

[40] Raymond, J. C., Kohl, J. L., Noci, G., et al., (1997), Composition of Coronal Streamers from the SOHO Ultraviolet Coronagraph Spectrometer, Solar Physics, Volume 175, Issue 2, pp 645–665.

[41] Cranmer S. R., Panasyuk A. V., Kohl J. L., (2008), The Astrophysical Journal, 678, 1480.

[42] Wilhelm K., Marsch E., Dwivedi B. N., Hassler D. M., Lemaire P., Gabriel A. H., Huber M. C., (1998) The solar corona above polar coronal holes as seen by SUMER on SOHO. The Astrophysical Journal, 500, 1023.

[43] Kohl J., Noci, G. and Antonucci, E., et al., (1997), The First Results from SOHO. Springer, pp 613–644.

[44] Cranmer S. R., Panasyuk A. V., Kohl J. L., (2008), The Astrophysical Journal, 678, 1480.

[45] Esser R., Fineschi S., Dobrzycka D., Habbal S. R., Edgar R. J., Raymond J. C., Kohl J. L., Guhathakurta M., 1998. Plasma properties in coronal holes derived from measurements of minor ion spectral lines and polarized white light intensity. The Astrophysical Journal Letters, 510, L63.

[46] Devlen E., Zengin Çamurdan D., Yardımcı M., Pekünlü E. R., (2017), A new model for heating of the Solar North Polar Coronal Hole. Monthly Notices of the Royal Astronomical Society, 467, 133-144.

[47] Hollweg J. V., 1999. Kinetic Alfvén wave revisited. Journal of Geophysical Research: Space Physics, 104, 14811-14819.

[48] Priest E. R., 1987. Solar magneto-hydrodynamics. D. Reidel Pub. Co.

[49] Spitzer Jr L., 1962. Physics of Fully Ionized Gases 2nd edition Interscience. New York.

[50] Doğan, S., Pekünlü, E. R., (2012), Ion-cyclotron waves in solar coronal hole, New Astronomy, Volume 17, Issue 3, p. 316-324.

[51] Hollweg, J. V., (1986), Transition region, corona, and solar wind in coronal holes, Journal of Geophysical Research, Volume 91, Issue A4, p. 4111-4125.

[52] Hollweg J. V., Johnson W., 1988. Transition region, corona, and solar wind in coronal holes: Some two-fluid models. Journal of Geophysical Research: Space Physics, 93, 9547-9554.

[53] Withbroe G. L., Noyes R. W., 1977. Mass and energy flow in the solar chromosphere and corona. Annual review of astronomy and astrophysics, 15, 363-387.

[54] McIntosh, S. W., de Pontieu, B., Carlsson, M., Hansteen, V., Boerner, P., Goossens, M., (2011), Alfvénic waves with sufficient energy to power the quiet solar corona and fast solar wind, Nature, Volume 475, Issue 7357, pp. 477-480.

[55] Cranmer, S. R., Matthaeus, W. H., Breech, B. A., Kasper, J. C., (2009), Empirical Constraints on Proton and Electron Heating in the Fast Solar Wind, The Astrophysical Journal, Volume 702, Issue 2, pp. 1604-1614.

[56] Hahn, M., Landi, E., Savin, D. W., (2012), Evidence of Wave Damping at Low Heights in a Polar Coronal Hole, The Astrophysical Journal, Volume 753, Issue 1, article id. 36, 9 pp.

[57] Hahn, M., Savin, D. W., (2013), Observational Quantification of the Energy Dissipated by Alfvén Waves in a Polar Coronal Hole: Evidence that Waves Drive the Fast Solar Wind, The Astrophysical Journal, Volume 776, Issue 2, article id. 78, 10 pp.

[58] Antonucci E., Dodero M. A., Giordano S., 2000. Oxygen temperature anisotropy and solar wind heating above coronal holes out to 5 R. Solar Physics, 197, 115-134.

[59] Telloni D., Antonucci E., Dodero M. A., 2007. Oxygen temperature anisotropy and solar wind heating above coronal holes out to 5 R. The Astronomy and Astrophysics, 476, 1341-1346.